ISG20L2, a Novel Vertebrate Nucleolar Exoribonuclease Involved in Ribosome Biogenesis*[S]

Yohann Couté‡§¶, Karine Kindbeiter‖, Stéphane Belin§**, Régis Dieckmann‡ ‡‡, Laurent Duret§§, Laurent Bezin¶¶, Jean-Charles Sanchez‡, and Jean-Jacques Diaz§‖‖

Proteomics analyses of human nucleoli provided molecular bases for an understanding of the multiple functions fulfilled by these nuclear domains. However, the biological roles of about 100 of the identified proteins are unpredictable. The present study describes the functional characterization of one of these proteins, ISG20L2. We demonstrate that ISG20L2 is a 3′ to 5′ exoribonuclease involved in ribosome biogenesis at the level of 5.8 S rRNA maturation, more specifically in the processing of the 12 S precursor rRNA. The use of truncated forms of ISG20L2 demonstrated that its N-terminal half promotes the nucleolar localization and suggested that its C-terminal half bears the exoribonuclease activity. Identification of the binding partners of ISG20L2 confirmed its involvement in the biogenesis of the large ribosomal subunit. These results strongly support the notion that, in human, as it was demonstrated in yeast, 5.8 S rRNA maturation requires several proteins in addition to the exosome complex. Furthermore this observation greatly sustains the idea that the extremely conserved need for correctly processed rRNAs in vertebrates and yeast is achieved by close but different mechanisms. ***Molecular & Cellular Proteomics 7:546–559, 2008.***

Nuclei of eukaryotic cells are highly organized organelles in which more than 30 different kinds of transient structures, called nuclear domains or nuclear bodies, support the nuclear functions (1). Since the 1960s, it has been known that nucleoli, the most prominent of the nuclear domains, are the sites of ribosome biogenesis. This function gives rise to their characteristic ultrastructural organization in three main compartments, the fibrillar center and the dense fibrillar and granular components (2).

Ribosome biogenesis is a very complex process that involves the synthesis of ribosomal RNAs (rRNAs)[1] coupled with their extensive processing, the assembly of these rRNAs with ribosomal proteins, and the export of the resulting preribosomal subunits from nuclei to cytoplasm where the final maturation occurs (3). rRNA processing mainly consists of base modifications and cleavages (4). Precursor rRNAs (pre-rRNAs) contain external and internal sequences that are not present within mature rRNAs. Removal of these sequences is achieved through sequential endonucleolytic and exonucleolytic cleavages, producing mature 18 S, 5.8 S, and 28 S rRNAs. Studies in yeast have identified several factors responsible for such cleavages: the ribonucleoprotein complex RNase MRP and Ngl2p catalyzing endoribonucleolytic processing, Xrn1p and Rat1p that are 5′ to 3′ exonucleases, Rex1p and Rex2p that are 3′ to 5′ exonucleases, and a protein complex named exosome composed of 3′ to 5′ exoribonucleases and putative RNA-binding proteins (5–9). However, the list of the catalytic factors required for the complete processing of pre-rRNAs into mature species is still incomplete.

Correct rRNA maturation that provides finely folded and packaged mature rRNAs is crucial because it is highly probable that eukaryotic ribosomes are, as it has clearly been demonstrated for prokaryote ribosomes, ribozymes (10, 11). In yeast, incorrectly maturated rRNAs lead to translational infidelity of ribosomes (12). In mammals, defects in pre-rRNA processing are therefore likely to entail the development of severe pathologies. Indeed results on *DKC1*, the gene altered in dyskeratosis congenita, indicated that altered rRNA processing plays a direct role in tumorigenesis (13). Recently Gleizes and co-workers (14) showed that ribosome biogenesis and notably pre-rRNA processing were altered in skin

From the ‡Biomedical Proteomics Research Group, Département de Biologie Structurale et Bioinformatique, Centre Médical Universitaire, 1 Rue Michel Servet, 1211 Geneva 4, Switzerland, §Centre de Génétique Moléculaire et Cellulaire (CNRS, UMR5534), 16 rue Dubois, §§Laboratoire de Biométrie et Biologie Evolutive (CNRS, UMR5558), 43 boulevard du 11 novembre 1918, and ¶¶Physiologie Intégrative Cellulaire et Moléculaire (CNRS, UMR5123), Bât Dubois, Université Lyon 1, 69622 Villeurbanne, France, and ‖Idéalp' Pharma, 66 boulevard Niels Bohr, Bât. CEI-BP 2132, 69603 Villeurbanne Cedex, France

Received, October 22, 2007, and in revised form, November 30, 2007

Published, MCP Papers in Press, December 6, 2007, DOI 10.1074/mcp.M700510-MCP200

[1] The abbreviations used are: rRNA, ribosomal RNA; pre-rRNA, precursor rRNA; ISG20L2, interferon-stimulated 20-kDa exonuclease-like 2; DAPI, 4′,6-diamidino-2-phenylindole; co-IP, co-immunoprecipitation; siRNA, small interfering RNA; aa, amino acids; EGFP, enhanced green fluorescent protein; mRNA, messenger RNA; hnRNP, heterogeneous nuclear ribonucleoprotein; PARN, poly(A)-specific ribonuclease.

TABLE I
Sequences of the primers used for plasmid constructions

Primer	Sequence
Q9H9L3up247	5′-TACGAATTCGCCTTCCATTGTCCCTATGTC-3′
Q9H9L3lo1383	5′-GAGGGATCCGAGCTGTCCATTGGTCCACT-3′
Q9H9L3Up3	5′-TGTAAGCTTTAGGATCCATGTCTACTTTACTGCTCAATCTG-3′
Q9H9L3Low3	5′-AGTGAATTCGAGCTGTCCATTGTCCAC-3′
Q9H9L3MidLow	5′-GGTGAATTCCTATGGCAACTTCTGGGATGCTC-3′
Q9H9L3MidUp	5′-AGTAAGCTTTAGGATCCTTGCCACGGAAGATGGTGGCA-3′
Q9H9L3MidLow2	5′-GGTGGATCCCTATGGCAACTTCTGGGATGCTC-3′
Q9H9L3Low1	5′-GGCAGATCTTCTAGATCCGGTGGATCCGA-3′

fibroblasts from patients suffering from Diamond-Blackfan anemia. More generally, defects in the biogenesis of ribosome components might play a major role in cancer (15, 16).

Ribosome biogenesis requires the contribution of more than 150 accessory factors that are not part of the ribosome itself (17, 18). In yeast, functional genomics and proteomics analyses allowed grouping these factors together into functional complexes that associate and dissociate sequentially from the preribosomal subunits during their maturation (19–21). In higher eukaryotes, however, most of the equivalent ortholog complexes remain to be characterized (22). Furthermore several specific factors regulating ribosome biogenesis in higher eukaryotes have yet to be identified. Knowledge of such proteins is of major interest to decipher the molecular mechanisms underlying ribosome biogenesis in higher eukaryotes and their subsequent functions in gene expression regulation. Recently several proteomics analyses of human nucleoli led to the identification of more than 700 different proteins (23–26). Extensive bibliographic and bioinformatics analyses allowed the classification of the identified proteins into functional groups. Notably a role in ribosome biogenesis was proposed for about 170 of these proteins (22). However, from all these studies, it remains that no biological function could be accurately assigned to more than 100 proteins.

The present report describes the characterization of one of these latter proteins, named interferon-stimulated 20-kDa exonuclease-like 2 (ISG20L2; UniProt Knowledgebase accession number Q9H9L3). We show that ISG20L2 is a member of a vertebrate exonucleases family composed of four proteins, co-orthologs of yeast Rex4p. ISG20L2 accumulates within nucleoli of HeLa cells and exerts an exoribonucleolytic activity on RNAs from their 3′- to their 5′-end. ISG20L2 is composed of at least two functional domains, one at its N-terminal half allowing intracellular localization and association with the binding partners and the other at its C-terminal half bearing the 3′ to 5′ exoribonuclease activity. Overexpression of ISG20L2 induces a specific decrease of the level of the 12 S pre-rRNA, whereas silencing of ISG20L2 induces an accumulation of this intermediate. The identification of the proteins associated with ISG20L2 confirmed that this protein is involved in ribosome biogenesis and most probably in the biogenesis of the large ribosomal subunit. ISG20L2 is therefore a novel human exonuclease involved in ribosome biogenesis, participating in the removal of the internal transcribed spacer 2 of pre-rRNAs.

EXPERIMENTAL PROCEDURES

Phylogenetic Tree of the REX4 Gene Family—Homologs of the yeast Rex4 protein were searched (with BLASTP) in UniProt (Release 8) and in Ensembl (Release 34). We retained all homologs having a similarity score higher than or equal to the score of the yeast Rex1 paralog. Sequences were aligned with MUSCLE (27).

The phylogenetic tree was inferred from protein sequence alignments by maximum likelihood. We used Phyml (28, 29) under the Jones-Taylor-Thornton model of protein evolution (30) with site-to-site rate variation modeled on a discrete γ distribution (four categories, shape parameter α, and proportion of invariable sites estimated from the data). The robustness of the phylogenetic inference was estimated by bootstrap (100 replicates). The tree was rooted by using Rex1 proteins as an outgroup.

Plasmid Constructions—To generate pEGFP-ISG20L2, an ISG20L2 cDNA was generated by RT-PCR (OneStep RT-PCR kit, Qiagen) using total RNAs extracted from HeLa cells (RNeasy kit, Qiagen) and specific primers (Q9H9L3up247 and Q9H9L3lo1383, Genome Express). The obtained cDNA was inserted into pEGFP-C1 (Clontech) after EcoRI/BamHI digestion. The p3XFLAG-ISG20L2 plasmid was generated by inserting the same EcoRI/BamHI fragment into p3XFLAG-CMV-10 (Sigma). To generate pGST-ISG20L2, amplified ISG20L2 cDNA (primers Q9H9L3Up3 and Q9H9L3Low3) was inserted into pGEX-4T-1 (GE Healthcare) after BamHI/EcoRI digestion.

To generate deletion mutants of ISG20L2, cDNA fragments were amplified by PCR from pEGFP-ISG20L2 using the following primers: Q9H9L3Up3 and Q9H9L3MidLow for ISG20L2-N-ter and Q9H9L3MidUp and Q9H9L3Low3 for ISG20L2-C-ter. The obtained fragments were inserted into pEGFP-C1 after HindIII/EcoRI) digestion. The p3XFLAG-ISG20L2 plasmid was generated by inserting the same EcoRI/BamHI fragment into p3XFLAG-CMV-10 (Sigma). p3XFLAG-ISG20L2-N-ter and p3XFLAG-ISG20L2-C-ter were generated by inserting amplified cDNA fragments (primers Q9H9L3Up3 and Q9H9L3MidLow2 for ISG20L2-N-ter and Q9H9L3MidUp and Q9H9L3Low1 for ISG20L2-C-ter) into p3XFLAG-CMV-10 after BamHI digestion. To generate pGST-ISG20L2-N-ter, an amplified cDNA fragment (primers Q9H9L3Up3 and Q9H9L3MidLow) was inserted into pGEX-4T-1 after BamHI/EcoRI digestion. The sequences of the primers used are listed in Table I.

Culture Conditions and Transfection of HeLa Cells—HeLa cells were grown in Petri dishes in minimum essential medium supplemented with 5% fetal calf serum at 37 °C with 5% CO_2. Cells were transfected with plasmids using the Lipofectamine reagent (Invitrogen) according to the manufacturer's instructions.

Immunofluorescence Analyses—Cells were grown on glass cover-

slips and fixed with 4% paraformaldehyde in PBS before permeabilization with 1% Triton X-100 in PBS. B23 and coilin were localized using mouse monoclonal antibodies (B0556 and C1862, respectively; Sigma) and a FluoProbes 546 anti-mouse secondary antibody (Interchim). Coverslips were mounted using Vectashield mounting medium with DAPI (Vector Laboratories). Fluorescent fusion proteins, Texas Red-labeled antibody, and DAPI were visualized at room temperature by confocal microscopy using a Plan Apochromat 63× oil immersion lens (numerical aperture, 1.4) on an LSM 510 Meta upright microscope from Zeiss. Digital images were captured using an AxioCam HR camera and acquired using the LSM software (Zeiss). Images were processed using the AxioVision LE software (Zeiss).

In Vitro Exoribonuclease Assays—Recombinant GST fusion proteins were produced in JM109 bacteria (Promega) and purified from bacterial lysates by affinity chromatography on glutathione-Sepharose 4B beads (GE Healthcare) (31). Solutions of purified proteins were dialyzed against 10 mM Tris-HCl, pH 7.2.

End-labeled RNA substrates were prepared as described previously (9) from a RNA synthesized *in vitro* by T7 polymerase transcription of the pBS(SK+) plasmid (Stratagene) linearized with EcoRI. ^{32}P-labeled RNA substrates were incubated with proteins of interest (ratio of one molecule of RNA/five molecules of protein) at 37 °C in 10 mM Tris-HCl, pH 7.6, 50 mM KCl, 5 mM $MgCl_2$, 10 mM DTT, 0.8 units/μl RNasin (Promega), and 0.01% BSA. Reactions were stopped by the addition of 1 volume of formamide followed by incubation at 70 °C for 5 min. Samples were resolved by PAGE in 11% polyacrylamide gels, and the reaction products were visualized by autoradiography.

Immunoprecipitation Experiments—Cells were harvested 48 h after transfection. Cells in PBS were scraped off while on ice. From this stage, all experiments were performed at 4 °C. Cells were pelleted by centrifugation and resuspended in the lysis buffer (25 mM Tris-HCl, pH 8, 200 mM NaCl, 1% Triton X-100, 0.5% CHAPS, 0.3% Nonidet P-40, 0.2% SDS, 1 mM DTT, and antiproteases). After a 90-min incubation, lysates were submitted to 30-min centrifugation at 20,000 × *g*. Supernatants were then incubated overnight with the M2 anti-FLAG antibody (Sigma). Immunocomplexes were immobilized on Protein A-Sepharose beads (GE Healthcare) by a 30-min incubation. Beads were collected and washed five times with the lysis buffer. When necessary, RNase A was incubated with the sample during 10 min at 37 °C at a final concentration of 5 μg/ml of lysis buffer after the second wash and before the third wash. Protein complexes were directly eluted by adding Laemmli buffer and heating at 95 °C for 10 min. Proteins were resolved by SDS-PAGE and revealed by silver nitrate or colloidal Coomassie Blue (Bio-Rad) stainings.

In-gel Digestion and Protein Identification by Tandem Mass Spectrometry—In-gel digestion was performed as described by Scherl *et al.* (24). LC-MS/MS analysis with the LCQ ion trap (Thermo Finnigan, San Jose, CA) was performed as described by Burgess *et al.* (32). Peak lists were generated using Bioworks 3.1 software (Thermo Finnigan). The resulting .dta files from each analysis were automatically combined into a single text file. The resulting peak lists were searched against the UniProt Knowledgebase Swiss-Prot/TrEMBL database (version 9.4, restricted to Mammalia, 251,818 entries) for co-immunoprecipitation (co-IP) experiment analyses and against the UniProt Swiss-Prot database (version 51.4, 309,349 entries) for GST fusion protein analyses using Phenyx (version 2.3, Genebio, Geneva, Switzerland) and Mascot operating on a local server (version 2.1, Matrix Science, London, UK). With Phenyx, ion trap was selected as the instrument type, and LCQ was selected for the algorithm. Two search rounds were used, both with trypsin selected as the enzyme and oxidized methionine and carbamidomethylated cysteine selected as variable modifications. In the first round one missed cleavage was allowed, and the normal cleavage mode was used. This round was selected in "turbo" search mode. In the second round three missed cleavages were allowed, and the cleavage mode was set to half-cleaved. The minimum peptide length allowed was 6 amino acids, and the parent ion tolerance was 2.0 Da in both search rounds. The acceptance criteria were slightly lowered in the second round search (round 1: AC score, 7.0; peptide Z-score, 7.0, peptide *p* value, 1*e*−7; round 2: AC score, 7.0; peptide Z-score, 6.0; peptide *p* value, 1*e*−6). Mascot was used with average mass selected, a precursor mass error of 2.0 Da, and a peptide mass error of 1.0 Da. Trypsin was selected as the enzyme with three potential missed cleavages. ESI ion trap was selected as the instrument type, and oxidized methionine and carbamidomethylated cysteine were selected as variable modifications. Only proteins that were identified with one or more high scoring peptides from both Mascot and Phenyx were considered to be true matches. "High scoring peptides" corresponded to peptides that were above the threshold in Mascot (expect value <0.05) and Phenyx (*p* value >1*e*−7) searches. Spectra of unique peptide matching proteins are provided (see the supplemental data). All identified human proteins were checked manually to contain at least one specific and non-redundant peptide. When possible, to avoid redundancy, human proteins of the Swiss-Prot database were preferred. If identified peptides were not able to single out a protein of a multiprotein family (as is the case for one protein in this work) all the entries matching with the same set of peptides are indicated (see the supplemental table). Identified keratins, immunoglobulins, and trypsin have not been included.

ISG20L2 Silencing Using Small interfering RNA (siRNA)—An siRNA duplex oligoribonucleotide against ISG20L2, synthesized by Proligo, was used for ISG20L2 silencing. Its sequences were as follows: sense, 5′-CUCCACAUGUUGGACAGUAdTdT-3′; antisense, 5′-UACUGUCCAACAUGUGGAGdTdT-3′. The BLOCK-iT fluorescent oligo (Invitrogen) that is not homologous to any known genes was used as a transfection efficiency detector and a negative control to ensure against induction of nonspecific cellular events caused by introduction of the siRNA into cells. This oligonucleotide is a double-stranded RNA exhibiting a sequence that is not homologous to any known gene and coupled to FITC. HeLa Cells were transfected with siRNAs using Lipofectamine 2000 in serum-free Opti-MEM (Invitrogen) according to the manufacturer's instructions. Cells were harvested 48 h after transfection.

The efficiency of ISG20L2 silencing was measured using quantitative RT-PCR. For this, 1 μg of total RNA free of genomic DNA contamination was reverse transcribed in the presence of 200 units of Moloney murine leukemia virus reverse transcriptase, RNase H^- (Promega), a 0.5 mM concentration of each dNTP (Promega), 1 μg of $oligo(dT)_{15}$, and finally 10^7 copies of synthetic messenger RNA, an external and non-competitive synthetic poly(A) RNA. The cDNAs of interest were amplified by real time PCR performed on the LightCycler® 1.2 System (Roche Diagnostics) using the QuantiTect SYBR® Green PCR kit (Qiagen). The copy number of each cDNA of interest present in the PCR mixture before amplification was determined using a standard curve ranging from 10 to 10^8 copies of the amplified sequence. Primer sets were designed using the "Universal Probe Library" software (Roche Diagnostics). The amplification of the cDNA of the synthetic messenger RNA (so-called ScDNA) was used to normalize the RT between samples; this patented method avoids making reference to a housekeeping gene, the level of which is believed to be invariant (76).

Northern Blot Analyses—Sequences of the probes (Invitrogen) used for Northern blot analyses are as follows: 18 S, 5′-ATCGGCCCGAGGTTATCTAGAGTCACCAAA-3′; 28 S, 5′-CCTCTTCGGGGGACGCGCGCGTGGCCCCGA-3′; 5.8 S, 5′-TCAGACAGGCGTAGCCCCGGGAGGAACCCG-3′. For labeling, 50 pmol of each probe were incubated with 50 pmol of [γ-^{32}P]ATP and T4 polynucleotide kinase (Promega) during 30 min at 37 °C.

Northern hybridizations were performed as described previously

(33). For each experimental condition, the radioactivity contained in every band corresponding to known rRNA species was quantified using PhosphorImager (Typhoon, GE Healthcare) scanning. Statistical analysis (paired *t* test) from results obtained in independent experiments was performed using Prism 4 software (GraphPad Software).

RESULTS

In Silico Prediction of Potential Functional Domains of ISG20L2 and Phylogenetic Tree of the REX4 Gene Family—Proteomics analyses of nucleoli purified from human cells have led to the identification of more than 700 different proteins (23–26). Despite extensive bibliographic and bioinformatics analyses, the biological role of about 16% of these proteins was still unpredictable (22). ISG20L2 was one of these proteins.

Human ISG20L2 is the product of a gene localized on the minus strand of chromosome 1 at position 1q21.3 (GeneID 81875 in Entrez Gene). ISG20L2 is a protein composed of 353 amino acids (aa) with a theoretical molecular mass and an isoelectric point of 39 kDa and 9.9, respectively (ExPASy). Searches of potential functional domains of ISG20L2 using the InterPro database allowed pinpointing a potential exonuclease domain localized between aa 178 and 344 of the protein (Fig. 1*A*). This potential exonuclease domain contains the conserved motifs and important residues characteristic of the DEDDh group of the DEDD superfamily of exonucleases (34) (Fig. 1*A*).

A phylogenetic study showed that ISG20L2 belongs to the *REX4* gene family. The biological functions of the vast majority of the proteins contained in this family are not known except for the *Saccharomyces cerevisiae* protein Rex4 involved in ribosome biogenesis (35, 36), for a human nuclease, ISG20, involved in antiviral response (37, 38), and for another human protein, Rex4 (also called XPMC2H), shown to regulate quinone reductase gene transcriptional activity (39). To further analyze the *REX4* gene family, we searched sequence databases (and notably complete genome databases) for homologs of the yeast Rex4 protein. We retained all homologs having a similarity score higher than or equal to the score of the yeast Rex1 paralog. The phylogenetic tree (rooted with Rex1) indicates that the *REX4* gene is single copy in most eukaryotic taxa (fungi, alveolates, invertebrates, and Mycetozoa) (Fig. 1*B*). The only exceptions are plants and vertebrates that contain, respectively, three and four members of the Rex4 family. The four vertebrate genes are *REX4*, *ISG20*, *ISG20L1*, and *ISG20L2* (respectively, Q9GZR2, Q96AZ6, Q9BSA5, and Q9H9L3 entries in UniProt Knowledgebase). The four encoded proteins contain a highly similar version of the exonuclease domain (Fig. 1*C*). Because of weak bootstrap values, this phylogenetic tree does not allow a precise dating of the duplications that led to the four vertebrate genes. However, the fact that we found a single *REX4* gene in the complete genome of the urochordate *Ciona intestinalis* (the closest sister group of vertebrates) as well as in other invertebrates (nematodes and insects) strongly suggests that these duplications occurred in the last common ancestor of vertebrates after their divergence from other chordates. In other words, vertebrate Rex4, ISG20, ISG20L1, and ISG20L2 appear to be co-orthologs of the yeast Rex4 protein. The fact that ISG20, ISG20L1, and ISG20L2 appear in the phylogenetic tree to be more distant from Rex4 is likely due to a higher rate of evolution.

ISG20L2 Accumulates within Nucleoli of HeLa Cells—Proteomics analyses of nucleoli purified from human cells suggested that ISG20L2 was present in nucleoli (24–26). To confirm this observation and because no antibody directed against ISG20L2 was available, the intracellular distribution of ISG20L2 was investigated by detection of a fusion EGFP-ISG20L2 protein in HeLa cells. Localization studies using confocal fluorescence microscopy showed that EGFP-ISG20L2 was concentrated within the same nuclear domains as B23, a major nucleolar protein, and does not seem to accumulate in other cell compartments (Fig. 2*A*), notably Cajal bodies (Fig. 2*B*), contrary to ISG20 (40). These observations confirm that ISG20L2 is a nucleolar protein.

The N-terminal Half of ISG20L2 Is Sufficient for Its Nucleolar Localization—To determine which part of ISG20L2 is involved in its nucleolar localization, two different hybrid proteins containing parts of ISG20L2 fused to EGFP were expressed in HeLa cells. Fluorescence microscopy observations showed that the hybrid protein containing the N-terminal half (aa 1–176) was concentrated within nucleoli like endogenous B23 (Fig. 2*C*). The hybrid protein containing the C-terminal half (aa 175–353) was distributed throughout the entire nucleus (Fig. 2*D*). These results indicate that the N-terminal half of ISG20L2 is sufficient for the nucleolar accumulation of the entire protein, whereas the C-terminal half is not required for this event.

ISG20L2 Is a 3′ to 5′ Exoribonuclease—To determine experimentally whether ISG20L2 carries an exoribonuclease activity, GST-ISG20L2 and GST-ISG20L2-N-ter fusion proteins were produced in bacteria and purified by affinity chromatography (Fig. 3*A*). The purity of the isolated proteins was checked by SDS-PAGE, and their identities were confirmed using MS/MS (see the supplemental table). Unfortunately the production of a GST-ISG20L2-C-ter fusion protein has failed despite numerous trials (data not shown).

The purified proteins were then assayed for *in vitro* ribonuclease activity. For this, GST-ISG20L2 was incubated for different periods of time with an *in vitro* synthesized RNA labeled at its 5′-end with ^{32}P. As shown in Fig. 3*B*, this incubation induced a progressive and sequential appearance of RNA fragments visible as soon as 5 min after the beginning of the incubation. Thirty minutes after the beginning of the incubation with GST-ISG20L2, the original substrate was no more detectable. On the contrary, its incubation with GST alone or with GST-ISG20L2-N-ter did not lead to its fragmentation or its disappearance even after 60 min of incubation. These results demonstrate that ISG20L2 possesses a 3′ to 5′ exori-

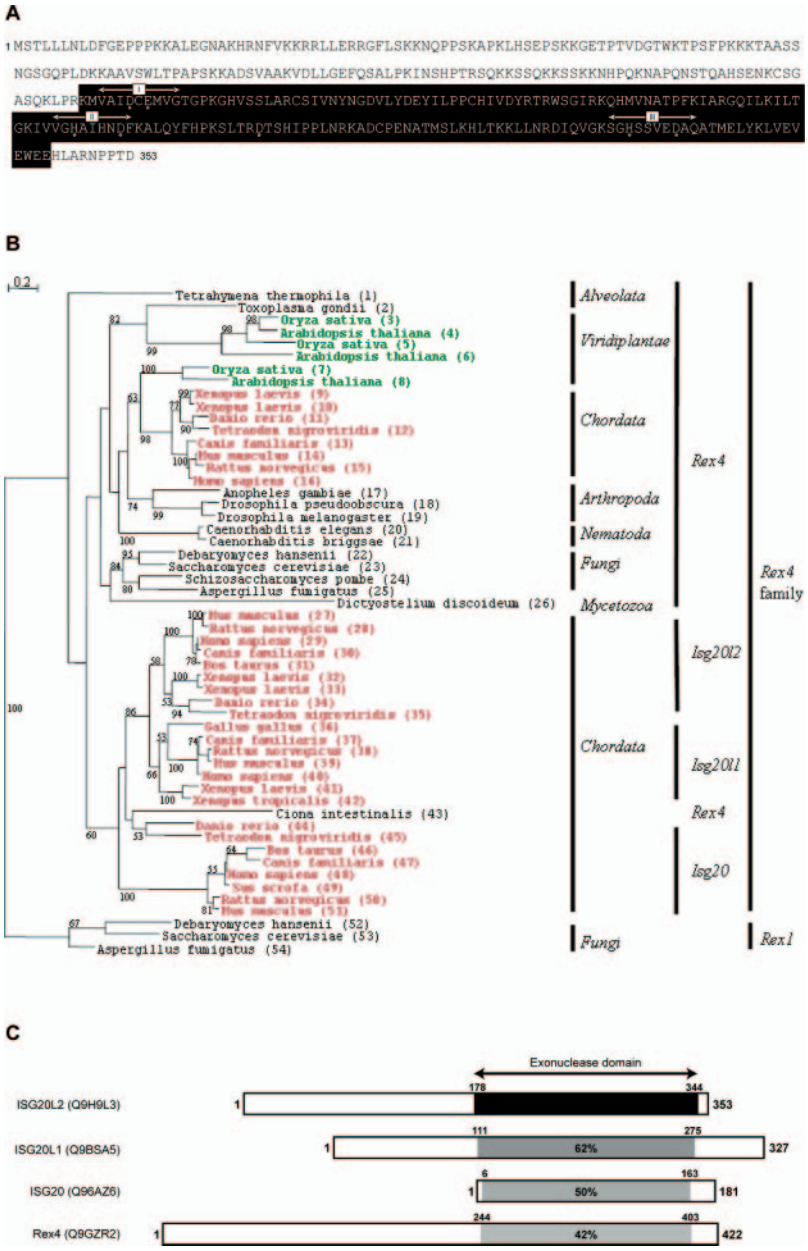

FIG. 1. **Bioinformatics analyses of ISG20L2 primary sequence and of the *REX4* gene family.** *A*, amino acid sequence of ISG20L2. The *in silico* predicted exonuclease domain is presented in a *black box* (amino acids 178–344); conserved motifs and important residues characteristic of the DEDDh exonuclease class are marked, respectively, by *white arrowheads* and *asterisks*. *B*, homologs of the yeast Rex4 protein were searched (with BLASTP) in UniProt and in Ensembl complete metazoan genomes. The tree is based on the multiple alignment of the conserved region (223 sites). The tree was rooted by using Rex1 as an outgroup. Bootstrap values higher than 50% are indicated. Vertebrate species are indicated in *red*; plant species are in *green*. UniProt or Ensembl accession numbers are as follows: *1*, Q22S54; *2*, Q5MAV6; *3*, Q8S3S6; *4*, Q700D3; *5*, Q9FTM4; *6*, Q8LE91; *7*, Q7F186; *8*, Q8LAA0; *9*, Q91560; *10*, Q2TAR2; *11*, ENSDARG00000044805; *12*, Q4SXK5; *13*, ENSCAFG00000019767; *14*, Q6PAQ4; *15*, ENSRNOG00000027867; *16*, Q9GZR2; *17*, Q7PQ12; *18*, Q2M084; *19*, Q9VUC3; *20*, Q9XXI3; *21*, Q60S67; *22*, Q6BIK6; *23*, Q08237; *24*, O94375; *25*, Q4WHF8; *26*, Q54U94; *27*, Q8BKA9; *28*, ENSRNOG00000030338; *29*, Q9H9L3; *30*, ENSCAFG00000016753; *31*, Q2YDK1; *32*, Q4V7K3; *33*, Q3B8G1; *34*, ENSDARG00000021179; *35*, Q4S474; *36*, ENSGALG00000006736; *37*, ENSCAFG00000011521; *38*, ENSRNOG00000018421; *39*, Q9CZI9; *40*, Q9BSA5; *41*, Q63ZS9; *42*, ENSXETG00000007588; *43*, ENSCING00000004431; *44*, ENSDARG00000045806; *45*, Q4SE83; *46*, ENSBTAG00000014762; *47*, ENSCAFG00000011525; *48*, Q96AZ6; *49*, Q66UW5; *50*, Q5RJP5; *51*, Q3UW00; *52*, Q6BJX1; *53*, P53331; *54*, Q4X025. *C*, human proteins containing an exonuclease domain highly similar to that of ISG20L2 are schematically represented. The position of the exonuclease domain is represented in each protein by a *gray box*, containing the percentage of identity between this domain and that of ISG20L2.

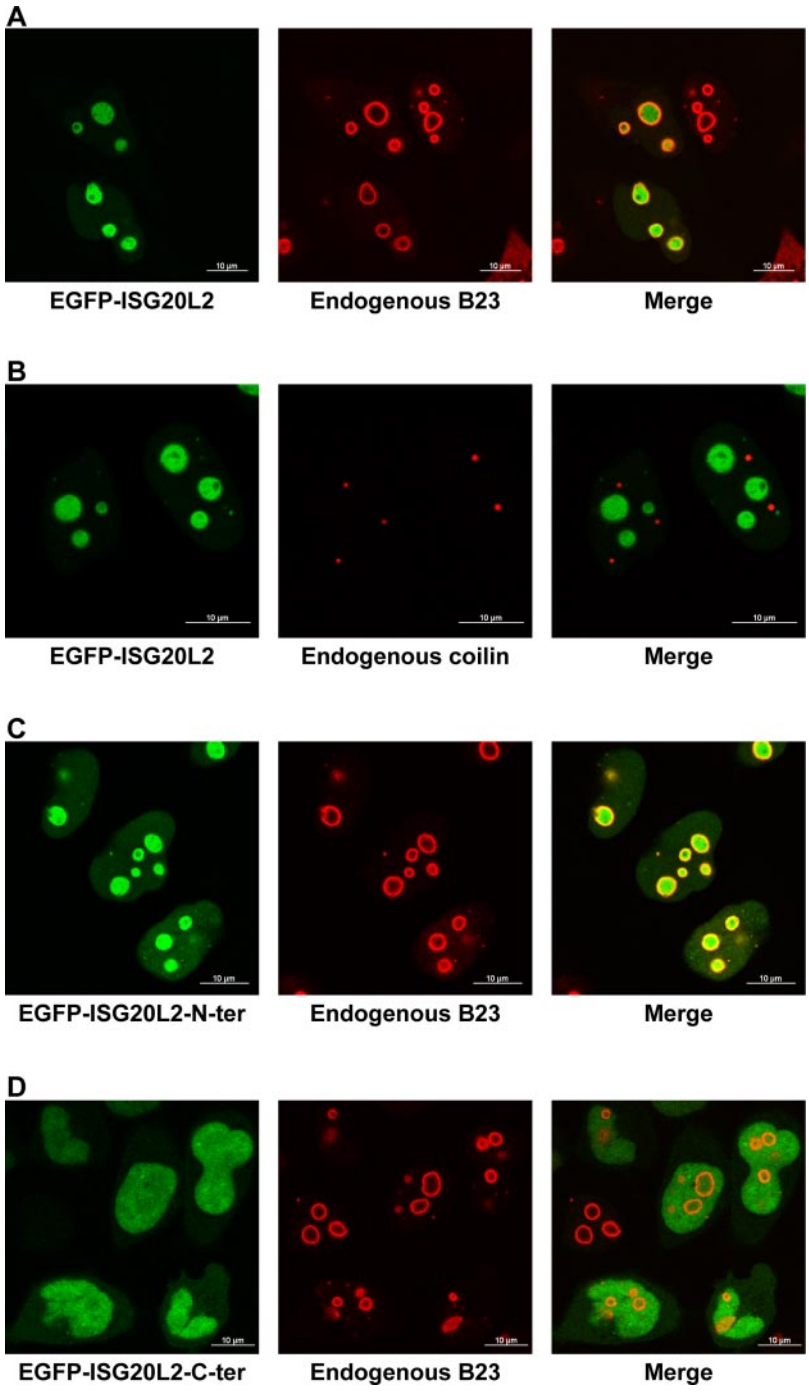

FIG. 2. **Intracellular localization of ISG20L2 and of ISG20L2 mutants.** EGFP-ISG20L2, EGFP-ISG20L2-N-ter (amino acids 1–176 of ISG20L2), and EGFP-ISG20L2-C-ter (amino acids 175–353 of ISG20L2) were transiently expressed in HeLa cells. Their intracellular localization was visualized by confocal microscopy on fixed cells. *A*, EGFP-ISG20L2 (*green*, *left panel*), endogenous B23 (*red*, *middle panel*), and merged signals (*right panel*); *B*, EGFP-ISG20L2 (*green*, *left panel*), endogenous coilin (*red*, *middle panel*), and merged signals (*right panel*); *C*, EGFP-ISG20L2-N-ter (*green*, *left panel*), endogenous B23 (*red*, *middle panel*), and merged signals (*right panel*); *D*, EGFP-ISG20L2-C-ter (*green*, *left panel*), endogenous B23 (*red*, *middle panel*), and merged signals (*right panel*).

bonuclease activity and that this activity is due to the exonuclease domain present in the C-terminal half of the protein.

To characterize the exoribonuclease activity more precisely, the fusion proteins were incubated with the same RNA but labeled with ^{32}P at its 3′-end instead of its 5′-end (Fig. 3, *C* and *D*). When the 3′ ^{32}P-labeled RNA was carrying a 3′-hydroxyl group, its incubation with GST-ISG20L2 led very rapidly to a dramatic decrease of the signal with no appearance of intermediates, whereas its incubation with GST and GST-ISG20L2-N-ter did not lead to this phenomenon (Fig. 3*C*). This confirms that ISG20L2 is a 3′ to 5′ exoribonuclease and suggests that it carries neither a 5′ to 3′ exoribonucleolytic nor an endoribonucleolytic activity. The fragmentation of the RNA induced by GST-ISG20L2 was prevented by the addition of a phosphate group at the 3′-end of the RNA (Fig. 3*D*). GST as well as GST-ISG20L2-N-ter did not degrade this type of RNA either (Fig. 3*D*). These results clearly demonstrate that ISG20L2 possesses a 3′ to 5′ exoribonuclease activity

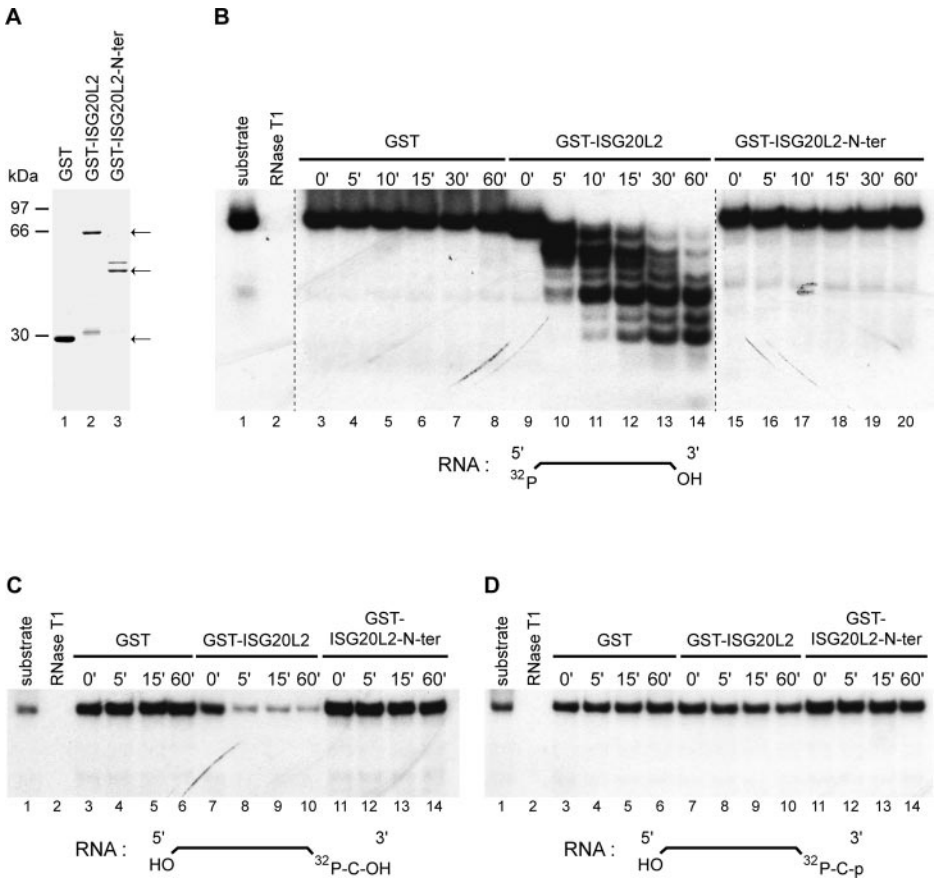

FIG. 3. **Assays of GST, GST-ISG20L2, and GST-ISG20L2-N-ter for exoribonuclease activity.** *A*, separation by SDS-PAGE and Coomassie Blue staining of 2.5 μg of affinity-purified GST, GST-ISG20L2, and GST-ISG20L2-N-ter. *Arrows* indicate the position of the respective proteins according to their identifications by Western blotting (data not shown) and MS/MS (supplemental table). *B*, *C*, and *D*, GST, GST-ISG20L2, and GST-ISG20L2-N-ter were assayed for exoribonuclease activity using *in vitro* synthesized RNAs in time course experiments. The RNA substrate was labeled with ^{32}P either at its 5′- (*B*) or 3′-end (*C* and *D*). The 3′-end of the substrate carried a hydroxyl group (*B* and *C*) or a phosphate group (*D*). The position of the radioactive label and the presence of terminal hydroxide or phosphate groups in each substrate are schematized *under* the corresponding panel. The substrate was incubated during 1 h in the assay buffer alone (*lane 1*) or with RNase T1 (*lane 2*) or during 0, 5, 10, 15, 30, and 60 min (*B*, *lanes 3–20*) or 0, 15, 30, and 60 min (*C* and *D*, *lanes 3–14*) with GST, GST-ISG20L2, or GST-ISG20L2-N-ter. The reaction products were separated by PAGE and visualized after autoradiography. *Dotted lines* indicate separate gels.

that displays a strong specificity for a 3′-end containing a free hydroxyl group.

ISG20L2 Associates with Ribosomal Proteins and Proteins Involved in Ribosome Biogenesis—To explore further the biological function of ISG20L2, the identification of its binding partners was achieved using 3XFLAG-tagged proteins. These fusion proteins exhibited the same localization patterns as the corresponding EGFP fusion proteins (Fig. 4, *A*, *B*, and *C*). The complexes containing 3XFLAG-ISG20L2 were purified by analytical co-IP using an anti-FLAG monoclonal antibody. To point out the proteins associated specifically with ISG20L2, immunoprecipitates obtained from cells expressing 3XFLAG-ISG20L2 were compared with those obtained from cells transfected with the plasmid coding only for the 3XFLAG peptide. For this, proteins contained within both immunoprecipitates were resolved by SDS-PAGE. About 20 different proteins were detected in both lanes after silver nitrate staining (Fig. 4*D*, *lanes 1* and *2*) and thus cannot be considered as specifically associated with ISG20L2. On the contrary, 20 other proteins were co-immunoprecipitated only in cells expressing 3XFLAG-ISG20L2 and can thus be considered as specific partners of ISG20L2. In addition RNase A treatment of the immunoprecipitated complexes showed that some of the interactions were RNA-dependent (supplemental Fig. 1). To identify the proteins associated with ISG20L2, a preparative co-IP was performed using approximately 100 times more cells than for the analytical co-IP. The immunoprecipitates were analyzed by SDS-PAGE, and the proteins were detected by colloidal Coomassie Blue staining (Fig. 4*E*, *lane 1*). The pattern of ISG20L2-binding proteins was very similar whether they were obtained from analytical or preparative co-IPs (Fig. 4, compare *D*, *lane 2* with *E*, *lane 2*), indicating that ISG20L2 is associated with the same proteins in both conditions. Proteins contained in each band were identified using MS/MS (supplemental table). This allowed the unambiguous identification of 18 different proteins associated with 3XFLAG-ISG20L2: three proteins involved in ribosome biogenesis (nucleolin, nucleolar RNA helicase II, and B23), 11 ribosomal proteins of the 60 S subunit, and four ribosomal proteins of the 40 S subunit (Fig. 4*E*, *lane 2*, and the supplemental table).

ISG20L2 and Its N-terminal Half Associate with the Same Proteins—EGFP-ISG20L2 and EGFP-ISG20L2-N-ter localized within nucleoli, whereas EGFP-ISG20L2-C-ter did not accumulate within these nuclear domains. It is now admitted that the precise intranuclear localization of a protein is not governed by specific sequences such as those allowing its nuclear import but is dependent on interactions with binding partners within the nucleus (41). Therefore the proteins specifically associated with ISG20L2, ISG20L2-N-ter, and ISG20L2-C-ter were compared. For this, analytical co-IP ex-

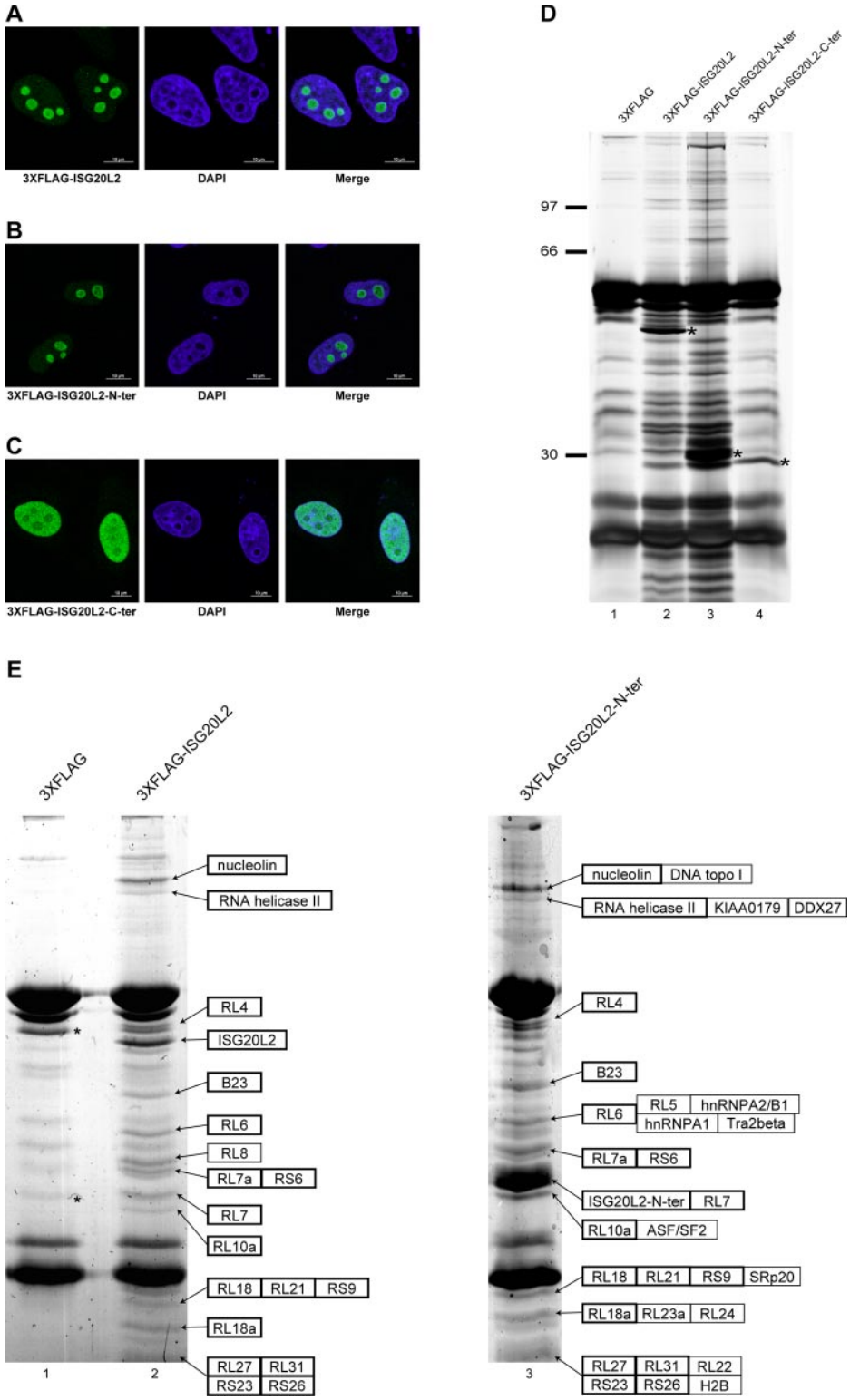

FIG. 4. **Co-immunoprecipitation and identification of the binding partners of ISG20L2.** 3XFLAG-ISG20L2 (*A*, *green*), 3XFLAG-ISG20L2-N-ter (*B*, *green*), and 3XFLAG-ISG20L2-C-ter (*C*, *green*) were transiently expressed in HeLa cells, and their intracellular localization was visualized by confocal microscopy on fixed cells; DAPI (*blue*) was used to stain the nucleus. *D*, analytical co-immunoprecipitation experiments. Proteins of the 3XFLAG-ISG20L2-, 3XFLAG-ISG20L2-N-ter-, and 3XFLAG-ISG20L2-C-ter-containing macromolecular complexes were separated by SDS-PAGE and revealed by silver nitrate staining (*lanes 2*, *3*, and *4*). A parallel experiment was performed as a control using cells expressing only the 3XFLAG peptide (*lane 1*). *E*, preparative co-immunoprecipitation experiments. Proteins co-immunoprecipitated specifically with 3XFLAG-ISG20L2 (*lane 2*) and 3XFLAG-ISG20L2-N-ter (*lane 3*) were identified using MS/MS. Names of the proteins identified as partner of ISG20L2 or ISG20L2-N-ter are indicated at the *right sides* of the lanes. Protein names in *bold* indicate that the corresponding proteins were identified as associated with ISG20L2 and ISG20L2-N-ter. Two bands (*) from control *lane 1* were subjected to in-gel digestion and MS/MS analyses, leading to the identification of immunoglobulin and trypsin (supplemental table).

periments were undertaken using an anti-FLAG antibody on lysates of HeLa cells transiently expressing 3XFLAG alone, 3XFLAG-ISG20L2, 3XFLAG-ISG20L2-N-ter, and 3XFLAG-ISG20L2-C-ter. The immunoprecipitates were separated by SDS-PAGE, and proteins were revealed by silver nitrate staining (Fig. 4*D*). The patterns of proteins specifically associated with ISG20L2 and with ISG20L2-N-ter were very similar, whereas no specific binding partners of 3XFLAG-ISG20L2-C-ter were observed. These results indicate that the N-terminal half of ISG20L2 probably interacts with the same partners as

the entire protein. As for ISG20L2, the interaction of ISG20L2-N-ter with some of its partners appeared to be dependent on RNA (supplemental Fig. 1). To further compare the proteins associated with ISG20L2 and ISG20L2-N-ter, a preparative co-IP of ISG20L2-N-ter and its partners was performed (Fig. 4*E*, *lane 3*). MS/MS analyses allowed the identification of 30 different proteins associated with 3XFLAG-ISG20L2-N-ter (six proteins involved or potentially involved in ribosomal biogenesis (nucleolin, nucleolar RNA helicase II, B23, DNA topoisomerase I, DDX27, and KIAA0179), 14 ribosomal proteins of the 60 S subunit, four ribosomal proteins of the 40 S subunit, five proteins involved in messenger RNA (mRNA) metabolism (hnRNP A1, hnRNP A2/B1, ASF/SF2, SRp20, and Tra2β), and histone H2B (Fig. 4*E*, *lane 3*, and the supplemental table). These results show that ISG20L2-N-ter is associated with the same partners as the entire protein and that it is able to reveal additional binding partners, notably proteins involved in mRNA metabolism.

Overexpression of ISG20L2 Induces a Specific Decrease of the 12 S Precursor rRNA, whereas ISG20L2 Silencing Induces a Specific Increase of the 12 S Precursor rRNA—With the aim of determining whether ISG20L2 could interfere with the rRNA synthesis pathway, the profiles of rRNA precursors as well as those of mature rRNAs were analyzed by Northern blots after overexpression of a recombinant form of ISG20L2 or after ISG20L2 silencing in HeLa cells. For this, on the one hand, HeLa cells were transfected with expression vectors coding for either EGFP or EGFP-ISG20L2, and, on the other hand, HeLa cells were transfected with either a control siRNA or an ISG20L2-specific siRNA (siISG20L2). Quantitative RT-PCR allowed us to demonstrate that, as expected, transfection of HeLa cells with siISG20L2 induced a specific decrease of the level of ISG20L2 mRNA of about 67% without affecting the levels of ISG20 and Rex4 mRNAs (ISG20L1 mRNA was not detectable; data not shown). Nuclear RNAs of cells over- and underexpressing ISG20L2 and of control cells were then purified and analyzed by Northern blot using a set of different radioactive probes allowing the detection of mature 5.8 S, 18 S, and 28 S rRNAs and of all their precursors that have been clearly identified in HeLa cells in previous studies (Fig. 5*A* and Ref. 42). Two of the Northern blot analyses performed with the 5.8 S probe are presented in Fig. 5, *B* and *C*. The data obtained from cells expressing EGFP-ISG20L2 or transfected with siISG20L2 were standardized in percentages to that of the corresponding control cells. The mean of these percentages as well as the corresponding S.D. were calculated from four (overexpression) and three (silencing) independent experiments (Fig. 5, *B* and *C*). The only statistically significant variations in correlation with the expression of EGFP-ISG20L2 or with ISG20L2 silencing were that observed for the 12 S rRNA precursor ($p = 0.0002$ and $p = 0.0168$, respectively). In cells expressing EGFP-ISG20L2, the amount of the 12 S pre-rRNA decreased by about 25% compared with that of cells expressing only EGFP, whereas the amount of the other precursors (45 S′, 41 S, and 32 S) and that of the 5.8 S rRNA was almost equivalent in both types of cells (Fig. 5*B*). In cells overexpressing ISG20L2, a precursor slightly longer than 5.8 S rRNA accumulated (Fig. 5*B*, *black arrowhead*). On the contrary, ISG20L2 silencing induced an increase of about 34% of the amount of the 12 S pre-rRNA compared with that measured in the control cells (Fig. 5*C*). Silencing of ISG20L2 did not modify significantly the amount of other pre-rRNAs or rRNAs, although we observed an important increase of the 45 S′ pre-rRNA amount. However, this increase was variable from one experiment to another and therefore was not considered statistically significant ($p > 0.05$).

DISCUSSION

ISG20L2 Is a Nucleolar 3′ to 5′ Exoribonuclease, a Member of a Family of Vertebrate Nucleolar Exonucleases—Proteomics analyses identified ISG20L2 as a component of nucleoli purified from human cells (24–26). The present work presents evidences that ISG20L2 is a 3′ to 5′ exoribonuclease found concentrated within nucleoli. As our attempts to produce an anti-ISG20L2 antibody were unsuccessful until now (data not shown), localization studies were performed using tagged proteins. Analyses of the localization of the fusion proteins EGFP-ISG20L2 as well as 3XFLAG-ISG20L2 using confocal microscopy revealed that ISG20L2 accumulates within nucleoli of HeLa cells. Furthermore a truncated form of ISG20L2 lacking its C-terminal half was still able to accumulate within nucleoli as did the entire protein. These results suggest that the N-terminal half of ISG20L2 probably promotes the nucleolar localization of the entire protein.

Bioinformatics studies revealed that, in its C-terminal half, ISG20L2 contains an exonuclease domain conserved in the DEDDh group of the DEDD superfamily of exonucleases. This group contains several RNases such as RNase T, oligoribonuclease, Rex proteins, the poly(A)-specific ribonuclease (PARN), and the poly(A) ribonuclease PAN2 as well as DNases such as DNA polymerase III that share a common catalytic mechanism characterized by the involvement of two metal ions (34, 43). The RNases of the DEDDh group are involved in various biological functions: RNase T is involved in the end turnover of tRNA and 3′ maturation of tRNAs, 5 S and 23 S rRNAs, and other small stable RNAs in *Escherichia coli* (44–48); oligoribonuclease is specific for small oligoribonucleotides and is involved in the mRNA decay pathway (49, 50); the Rex proteins Rex1p, Rex2p, and Rex3p operate in the 3′-end processing of rRNAs, transfer RNAs, MRP RNA, RNase P RNA, and small nuclear RNAs (8); and PARN and PAN2 are involved in mRNA turnover by degrading mRNA poly(A) tails (51, 52). Despite all these RNases belonging to the same group of exonucleases, they differ in their mode of action. Indeed oligoribonuclease and PARN were described as processive enzymes, whereas RNase T and PAN2 were shown to be non-processive enzymes (49, 53–55). Biochemical evidence demonstrates here that ISG20L2 is also an exoribo-

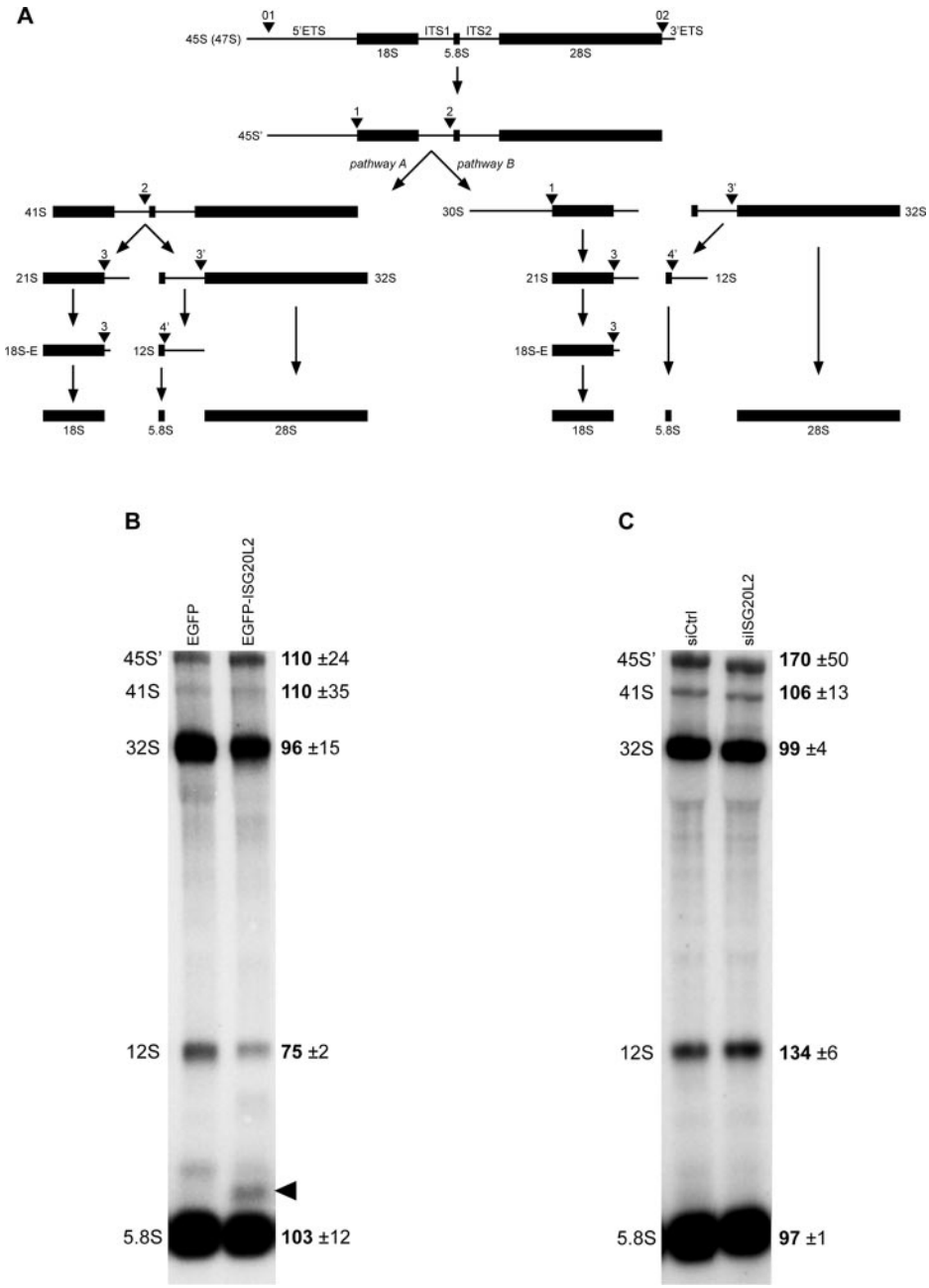

FIG. 5. **Effects of overexpression and silencing of ISG20L2 on the 5. 8 S rRNA maturation pathway.** *A*, schematic representation of rRNA processing in HeLa cells according to Ref. 42. Two alternative pathways are presented. *B* and *C*, Northern blot analysis of nuclear RNAs extracted from HeLa cells. Nuclear RNAs extracted from cells expressing EGFP or EGFP-ISG20L2 (*B*) and cells transfected with control siRNA or siISG20L2 (*C*) were detected by hybridization with a 5.8 S probe. Average intensities measured for rRNAs extracted from cells expressing EGFP-ISG20L2 (four independent experiments) and transfected with siISG20L2 (three independent experiments) are expressed as percentages of the intensities obtained with control cells. Standard deviations are given after the ± symbol. *siCtrl*, BLOCK-iT fluorescent oligo.

nuclease that processes RNAs from their 3′-end to their 5′-end. Processing of RNAs by ISG20L2 is characteristic of a distributive mode of hydrolysis because its incubation with a 5′-end-labeled RNA substrate generated fragments that were progressively shortened from its 3′-end. Furthermore our experiments indicated that ISG20L2 exhibits a strong preference for a 3′-hydroxyl group at the 3′-end of its substrate to achieve its exoribonuclease activity as it was described for RNase T and PARN (51, 56).

Phylogenetic studies indicated that ISG20L2 is a member of the Rex4 family in the Rex subgroup of DEDDh exonucleases. The Rex4 family is composed of three other members in vertebrates (Rex4, ISG20, and ISG20L1), probably after duplications of the *REX4* gene in the last common ancestor of vertebrates. These four proteins contain a very similar version of the exonuclease domain. ISG20 was characterized as a divalent processive cation-dependent 3′ to 5′ exonuclease with a strong preference for single-stranded RNA substrates accumulating in nucleoli but also in Cajal bodies (40, 57). Rex4 probably accumulates within nucleoli because it was identified in all proteomics analyses of nucleoli purified from human cells (23–26). A transiently expressed EGFP-ISG20L1 fusion protein accumulated also within nucleoli of HeLa cells (data not shown). In conclusion, ISG20, ISG20L1, ISG20L2, and

Rex4 are four vertebrate exonucleases of the same family that accumulate within nucleoli; the precise biological role of each member of the family in this nuclear domain remains to be specified.

ISG20L2 interacts with Ribosomal Proteins and Proteins Involved in Ribosome Biogenesis—To gain insights into the biological role of ISG20L2, identification of its binding partners was undertaken. Eighteen different proteins with which it associates were identified after co-IP experiments and MS/MS analyses. As it was described for other nucleolar proteins, the interaction of ISG20L2 with some of its partners appears to be dependent on RNA integrity, although the interactions between each member of the ISG20L2 complex, either RNA or proteins, remains to be finely deciphered (58–60). All the identified partners of ISG20L2 (except RS26) have been identified as localized within nucleoli of HeLa cells (22). Three of them are *trans*-acting factors involved in ribosome biogenesis: nucleolin, B23, and nucleolar RNA helicase II. Although the role of nucleolin in ribosome biogenesis is not fully understood, it is implicated in multiple steps during this pathway (61). B23 is a multifunctional nucleolar protein that may essentially act as an assembly factor of ribosomal subunits (62). Nucleolar RNA helicase II is involved in 18 S and 28 S rRNA production in mammals (63). Fifteen of the proteins identified as partners of ISG20L2 are ribosomal proteins, and notably 11 of them are part of the large ribosomal subunit. These findings and the fact that ISG20L2 localized within nucleoli of HeLa cells strongly suggest that ISG20L2 could be involved in ribosome biogenesis and most likely in the processing and assembly of the large ribosomal subunit.

The co-IP experiments revealed that ISG20L2 and its N-terminal half associate with the same binding partners, mainly proteins involved in ribosome biogenesis and ribosomal proteins. Indeed 30 different proteins were identified as associated with the N-terminal half of ISG20L2. Six of them are involved in ribosome biogenesis: nucleolin, B23, nucleolar RNA helicase II, DNA topoisomerase I, KIAA0179, and DDX27. DNA topoisomerase I is involved in pre-rRNA synthesis (64). The biological roles of KIAA0179 and DDX27 are still unknown. However, they are, respectively, homologous to the yeast proteins Rrp1p and Drs1p involved in the biogenesis of the large ribosomal subunit (65, 66). Eighteen of the proteins identified as associated with ISG20L2-N-ter are ribosomal proteins, and 14 of them belong to the large ribosomal subunit. These data further support the notion that ISG20L2 is involved in the biogenesis of the large ribosomal subunit. Therefore, it can be postulated that ISG20L2 is composed of two main functional domains, one in the N-terminal half of the protein promoting its intracellular localization via the association with its partners and the other in the C-terminal half of the protein bearing the biochemical activity of ISG20L2.

Besides ribosomal proteins and proteins involved in ribosome biogenesis, five unexpected proteins were identified as partners of ISG20L2-N-ter. They are all involved in mRNA metabolism. Four of these proteins, hnRNP A1, hnRNP A2/B1, SRp20, and ASF/SF2, are plurifunctional factors involved in splicing and nucleocytoplasmic export or trafficking of mRNAs (67). Tra2β is involved in mRNA splicing (68). This result suggests that ISG20L2 might be involved in several biological processes as it has been demonstrated for other exonucleases of the DEDDh group of the DEDD superfamily of exonucleases. It is then conceivable that ISG20L2, apart from an involvement in ribosome biogenesis, may play an additional role in mRNA metabolism.

ISG20L2 Is Involved in the Maturation of the 5.8 S rRNA—Identification of the binding partners of ISG20L2 strongly suggested that this protein is involved in the biogenesis of the large ribosomal subunit. In addition, a role for ISG20L2 in ribosome biogenesis is supported by the finding that it leaves nucleoli after actinomycin D treatment (25). We provide evidence that ISG20L2 participates in the processing of internal transcribed spacer 2 because its overexpression induced a decrease in the amount of the 12 S pre-rRNA, whereas its silencing induced an increase in the quantity of this well identified precursor of the 5.8 S rRNA. In yeast, the maturation step from the counterpart of the 12 S rRNA precursor (7 S pre-rRNA) to the 5.8 S rRNA is performed through sequential steps achieved by different factors. Indeed the exosome is thought to provide the 5.8 S + 30 precursor from the 12 S pre-rRNA. This precursor is shortened to the 6 S (5.8 S + 8) pre-rRNA by Rrp6p and to the 5.8 S + 5 precursor by Rex1p and/or Rex2p. Finally the last few nucleotides are removed by Ngl2p, providing the mature 5.8 S rRNA (6). In humans, the maturation of the 5.8 S rRNA is still not well defined even if a human exosome complex has been characterized (69). This complex contains proteins similar to those found in the yeast complex. However, its exonuclease activity is conferred by the hydrolytic activity of the Rrp41-Rrp45 dimer, which exhibits no activity in yeast, indicating that the activity and regulation of the exosome might have diverged between yeasts and humans, notably concerning the maturation of the 5.8 S rRNA (70, 71). It was suggested that, as is the case in yeast, the exosome is required but not sufficient for a complete 3′-end maturation of the human 5.8 S rRNA (72). ISG20L2 is probably one of the factors involved in the processing of the 12 S pre-rRNA. The fact that overexpression of ISG20L2 induced a decrease in amount of the 12 S pre-rRNA and the appearance of a band above the 5.8 S rRNA that might correspond to the yeast 6 S rRNA strongly support this hypothesis. However, the molecular mechanisms by which this occurs remain to be determined. For example extensive characterization of an RNA species that accumulates above the 5.8 S rRNA after overexpression of ISG20L2 should help to determine whether the processing of the 12 S rRNA is reminiscent of that of its yeast counterpart.

Because the available exosome composition does not include ISG20L2 and none of the binding partners of ISG20L2 identified in this study are part of the exosome, ISG20L2 is probably not part of the exosome *per se*. ISG20L2 may then

be considered as a novel protein involved in the maturation of the 5.8 S rRNA in a step specific to vertebrates. At the mechanistic level, ISG20L2 might cleave directly through its exoribonuclease activity or indirectly the 12 S pre-rRNA just before or just after the action of the exosome. Alternatively ISG20L2 might be a positive regulator of the exosome, explaining the decrease in amount of the 12 S pre-rRNA when ISG20L2 was overexpressed and its decrease in amount when ISG20L2 was underexpressed. Because ISG20L2 is specific to vertebrates, this demonstrates that the machinery required for 5.8 S maturation is probably more complex in higher eukaryotes than in yeast and requires several proteins in addition to the exosome complex as it has been described with the characterization of MPP6, a human cofactor of the exosome (72).

Interestingly we observed an increase, although variable and not statistically significant, in the amount of 45 S′ pre-rRNA after underexpression of ISG20L2. A similar phenomena is frequently observed in yeast when the processing of the 60 S subunit is altered (18, 73, 74). The mechanisms by which this occurs is not yet elucidated, but altogether these observations strongly support the notion that in mammals, like in yeast, there is some form of negative feedback on the processing machinery when the ribosome biogenesis is altered (75).

It appears more and more that rRNAs are crucial players for a good quality of the cell translational activity (12). Our results indicate that probably many proteins involved in the processing and in the quality control of rRNAs remain to be identified and characterized. Furthermore these results confirm that the extremely conserved need for rRNAs in vertebrates and yeast is achieved by close but distinct mechanisms, opening the exciting possibility to discover modes of regulations that are unique to higher eukaryotic systems.

Acknowledgments—We are grateful to Drs. Jennifer A. Burgess and Alexander Scherl (Biomedical Proteomics Research Group, Geneva, Switzerland) for technical assistance in mass spectrometry experiments, to Dr. Pierre Lescuyer (Biomedical Proteomics Research Group, Geneva, Switzerland) for advice on statistical issues, and to Dr. Alice Lebreton (CNRS-Centre de Genetique Moleculaire, Gif-sur-Yvette, France) and Prof. Pierre-Emmanuel Gleizes (Laboratoire de Biologie Moléculaire des Eucaryotes, CNRS and Université Paul Sabatier, Toulouse, France) for critical reading of the manuscript. Confocal microscopy experiments were performed in the Bioimaging Core Facility (Faculté de Médecine, Geneva, Switzerland).

* The costs of publication of this article were defrayed in part by the payment of page charges. This article must therefore be hereby marked "*advertisement*" in accordance with 18 U.S.C. Section 1734 solely to indicate this fact.

S The on-line version of this article (available at http://www.mcponline.org) contains supplemental material.

¶ To whom correspondence should be addressed: Biomedical Proteomics Research Group, Département de Biologie Structurale et Bioinformatique, 1 Rue Michel Servet, 1211 Geneva 4, Switzerland. Tel.: 41-22-3795907; Fax: 41-22-346-87-58; E-mail: yohann.coute@medecine.unige.ch.

** Recipient of a fellowship from La Ligue Nationale Contre le Cancer.

‡‡ Present address: Dépt. de biochimie, Sciences II, 30 Quai Ernest Ansermet, CH-1211 Genève 4, Switzerland.

|||| A member of INSERM.

REFERENCES

1. Dundr, M., and Misteli, T. (2001) Functional architecture in the cell nucleus. *Biochem. J.* **356,** 297–310
2. Melese, T., and Xue, Z. (1995) The nucleolus: an organelle formed by the act of building a ribosome. *Curr. Opin. Cell Biol.* **7,** 319–324
3. Rouquette, J., Choesmel, V., and Gleizes, P. E. (2005) Nuclear export and cytoplasmic processing of precursors to the 40S ribosomal subunits in mammalian cells. *EMBO J.* **24,** 2862–2872
4. Olson, M. O., Dundr, M., and Szebeni, A. (2000) The nucleolus: an old factory with unexpected capabilities. *Trends Cell Biol.* **10,** 189–196
5. Schmitt, M. E., and Clayton, D. A. (1993) Nuclear RNase MRP is required for correct processing of pre-5.8S rRNA in Saccharomyces cerevisiae. *Mol. Cell. Biol.* **13,** 7935–7941
6. Faber, A. W., Van Dijk, M., Raue, H. A., and Vos, J. C. (2002) Ngl2p is a Ccr4p-like RNA nuclease essential for the final step in 3′-end processing of 5.8S rRNA in Saccharomyces cerevisiae. *RNA* **8,** 1095–1101
7. Henry, Y., Wood, H., Morrissey, J. P., Petfalski, E., Kearsey, S., and Tollervey, D. (1994) The 5′ end of yeast 5.8S rRNA is generated by exonucleases from an upstream cleavage site. *EMBO J.* **13,** 2452–2463
8. van Hoof, A., Lennertz, P., and Parker, R. (2000) Three conserved members of the RNase D family have unique and overlapping functions in the processing of 5S, 5.8S, U4, U5, RNase MRP and RNase P RNAs in yeast. *EMBO J.* **19,** 1357–1365
9. Mitchell, P., Petfalski, E., and Tollervey, D. (1996) The 3′ end of yeast 5.8S rRNA is generated by an exonuclease processing mechanism. *Genes Dev.* **10,** 502–513
10. Nissen, P., Hansen, J., Ban, N., Moore, P. B., and Steitz, T. A. (2000) The structural basis of ribosome activity in peptide bond synthesis. *Science* **289,** 920–930
11. Rodnina, M. V., Beringer, M., and Wintermeyer, W. (2007) How ribosomes make peptide bonds. *Trends Biochem. Sci*. **32,** 20–26
12. Baxter-Roshek, J. L., Petrov, A. N., and Dinman, J. D. (2007) Optimization of ribosome structure and function by rRNA base modification. *PLoS ONE* **2,** e174
13. Ruggero, D., Grisendi, S., Piazza, F., Rego, E., Mari, F., Rao, P. H., Cordon-Cardo, C., and Pandolfi, P. P. (2003) Dyskeratosis congenita and cancer in mice deficient in ribosomal RNA modification. *Science* **299,** 259–262
14. Choesmel, V., Bacqueville, D., Rouquette, J., Noaillac-Depeyre, J., Fribourg, S., Cretien, A., Leblanc, T., Tchernia, G., Dacosta, L., and Gleizes, P. E. (2007) Impaired ribosome biogenesis in Diamond-Blackfan anemia. *Blood* **109,** 1275–1283
15. Pandolfi, P. P. (2004) Aberrant mRNA translation in cancer pathogenesis: an old concept revisited comes finally of age. *Oncogene* **23,** 3134–3137
16. Amsterdam, A., Sadler, K. C., Lai, K., Farrington, S., Bronson, R. T., Lees, J. A., and Hopkins, N. (2004) Many ribosomal protein genes are cancer genes in zebrafish. *PLoS Biol.* **2,** E139
17. Kressler, D., Linder, P., and de La Cruz, J. (1999) Protein trans-acting factors involved in ribosome biogenesis in Saccharomyces cerevisiae. *Mol. Cell. Biol.* **19,** 7897–7912
18. Venema, J., and Tollervey, D. (1999) Ribosome synthesis in Saccharomyces cerevisiae. *Annu. Rev. Genet.* **33,** 261–311
19. Fatica, A., and Tollervey, D. (2002) Making ribosomes. *Curr. Opin. Cell Biol.* **14,** 313–318
20. Tschochner, H., and Hurt, E. (2003) Pre-ribosomes on the road from the nucleolus to the cytoplasm. *Trends Cell Biol.* **13,** 255–263
21. Fromont-Racine, M., Senger, B., Saveanu, C., and Fasiolo, F. (2003) Ribosome assembly in eukaryotes. *Gene* (*Amst*.) **313,** 17–42
22. Coute, Y., Burgess, J. A., Diaz, J. J., Chichester, C., Lisacek, F., Greco, A., and Sanchez, J. C. (2006) Deciphering the human nucleolar proteome. *Mass Spectrom. Rev.* **25,** 215–234
23. Andersen, J. S., Lyon, C. E., Fox, A. H., Leung, A. K., Lam, Y. W., Steen, H., Mann, M., and Lamond, A. I. (2002) Directed proteomic analysis of the human nucleolus. *Curr. Biol.* **12,** 1–11
24. Scherl, A., Coute, Y., Deon, C., Calle, A., Kindbeiter, K., Sanchez, J. C., Greco, A., Hochstrasser, D., and Diaz, J. J. (2002) Functional proteomic analysis of human nucleolus. *Mol. Biol. Cell* **13,** 4100–4109

25. Andersen, J. S., Lam, Y. W., Leung, A. K., Ong, S. E., Lyon, C. E., Lamond, A. I., and Mann, M. (2005) Nucleolar proteome dynamics. *Nature* **433,** 77–83
26. Vollmer, M., Horth, P., Rozing, G., Coute, Y., Grimm, R., Hochstrasser, D., and Sanchez, J. C. (2006) Multi-dimensional HPLC/MS of the nucleolar proteome using HPLC-chip/MS. *J. Sep. Sci.* **29,** 499–509
27. Edgar, R. C. (2004) MUSCLE: multiple sequence alignment with high accuracy and high throughput. *Nucleic Acids Res.* **32,** 1792–1797
28. Guindon, S., and Gascuel, O. (2003) A simple, fast, and accurate algorithm to estimate large phylogenies by maximum likelihood. *Syst. Biol.* **52,** 696–704
29. Guindon, S., Lethiec, F., Duroux, P., and Gascuel, O. (2005) PHYML Online—a web server for fast maximum likelihood-based phylogenetic inference. *Nucleic Acids Res.* **33,** W557–W559
30. Jones, D. T., Taylor, W. R., and Thornton, J. M. (1992) The rapid generation of mutation data matrices from protein sequences. *Comput. Appl. Biosci.* **8,** 275–282
31. Catez, F., Erard, M., Schaerer-Uthurralt, N., Kindbeiter, K., Madjar, J. J., and Diaz, J. J. (2002) Unique motif for nucleolar retention and nuclear export regulated by phosphorylation. *Mol. Cell. Biol.* **22,** 1126–1139
32. Burgess, J. A., Lescuyer, P., Hainard, A., Burkhard, P. R., Turck, N., Michel, P., Rossier, J. S., Reymond, F., Hochstrasser, D. F., and Sanchez, J. C. (2006) Identification of brain cell death associated proteins in human post-mortem cerebrospinal fluid. *J. Proteome Res.* **5,** 1674–1681
33. Henras, A., Henry, Y., Bousquet-Antonelli, C., Noaillac-Depeyre, J., Gelugne, J. P., and Caizergues-Ferrer, M. (1998) Nhp2p and Nop10p are essential for the function of H/ACA snoRNPs. *EMBO J.* **17,** 7078–7090
34. Zuo, Y., and Deutscher, M. P. (2001) Exoribonuclease superfamilies: structural analysis and phylogenetic distribution. *Nucleic Acids Res.* **29,** 1017–1026
35. Eppens, N. A., Faber, A. W., Rondaij, M., Jahangir, R. S., van Hemert, S., Vos, J. C., Venema, J., and Raue, H. A. (2002) Deletions in the S1 domain of Rrp5p cause processing at a novel site in ITS1 of yeast pre-rRNA that depends on Rex4p. *Nucleic Acids Res.* **30,** 4222–4231
36. Faber, A. W., Vos, J. C., Vos, H. R., Ghazal, G., Elela, S. A., and Raue, H. A. (2004) The RNA catabolic enzymes Rex4p, Rnt1p, and Dbr1p show genetic interaction with trans-acting factors involved in processing of ITS1 in Saccharomyces cerevisiae pre-rRNA. *RNA* **10,** 1946–1956
37. Gongora, C., David, G., Pintard, L., Tissot, C., Hua, T. D., Dejean, A., and Mechti, N. (1997) Molecular cloning of a new interferon-induced PML nuclear body-associated protein. *J. Biol. Chem.* **272,** 19457–19463
38. Espert, L., Degols, G., Gongora, C., Blondel, D., Williams, B. R., Silverman, R. H., and Mechti, N. (2003) ISG20, a new interferon-induced RNase specific for single-stranded RNA, defines an alternative antiviral pathway against RNA genomic viruses. *J. Biol. Chem.* **278,** 16151–16158
39. Montano, M. M., Wittmann, B. M., and Bianco, N. R. (2000) Identification and characterization of a novel factor that regulates quinone reductase gene transcriptional activity. *J. Biol. Chem.* **275,** 34306–34313
40. Espert, L., Eldin, P., Gongora, C., Bayard, B., Harper, F., Chelbi-Alix, M. K., Bertrand, E., Degols, G., and Mechti, N. (2006) The exonuclease ISG20 mainly localizes in the nucleolus and the Cajal (Coiled) bodies and is associated with nuclear SMN protein-containing complexes. *J. Cell. Biochem.* **98,** 1320–1333
41. Misteli, T. (2001) Protein dynamics: implications for nuclear architecture and gene expression. *Science* **291,** 843–847
42. Hadjiolova, K. V., Nicoloso, M., Mazan, S., Hadjiolov, A. A., and Bachellerie, J. P. (1993) Alternative pre-rRNA processing pathways in human cells and their alteration by cycloheximide inhibition of protein synthesis. *Eur. J. Biochem.* **212,** 211–215
43. Steitz, T. A., and Steitz, J. A. (1993) A general two-metal-ion mechanism for catalytic RNA. *Proc. Natl. Acad. Sci. U. S. A.* **90,** 6498–6502
44. Deutscher, M. P., Marlor, C. W., and Zaniewski, R. (1985) RNase T is responsible for the end-turnover of tRNA in Escherichia coli. *Proc. Natl. Acad. Sci. U. S. A.* **82,** 6427–6430
45. Li, Z., and Deutscher, M. P. (1996) Maturation pathways for E. coli tRNA precursors: a random multienzyme process in vivo. *Cell* **86,** 503–512
46. Li, Z., and Deutscher, M. P. (1995) The tRNA processing enzyme RNase T is essential for maturation of 5S RNA. *Proc. Natl. Acad. Sci. U. S. A.* **92,** 6883–6886
47. Li, Z., Pandit, S., and Deutscher, M. P. (1999) Maturation of 23S ribosomal RNA requires the exoribonuclease RNase T. *RNA* **5,** 139–146
48. Li, Z., Pandit, S., and Deutscher, M. P. (1998) 3′ exoribonucleolytic trimming is a common feature of the maturation of small, stable RNAs in Escherichia coli. *Proc. Natl. Acad. Sci. U. S. A.* **95,** 2856–2861
49. Niyogi, S. K., and Datta, A. K. (1975) A novel oligoribonuclease of Escherichia coli. I. Isolation and properties. *J. Biol. Chem.* **250,** 7307–7312
50. Ghosh, S., and Deutscher, M. P. (1999) Oligoribonuclease is an essential component of the mRNA decay pathway. *Proc. Natl. Acad. Sci. U. S. A.* **96,** 4372–4377
51. Astrom, J., Astrom, A., and Virtanen, A. (1992) Properties of a HeLa cell 3′ exonuclease specific for degrading poly(A) tails of mammalian mRNA. *J. Biol. Chem.* **267,** 18154–18159
52. Boeck, R., Tarun, S., Jr., Rieger, M., Deardorff, J.A., Muller-Auer, S., and Sachs, A. B. (1996) The yeast Pan2 protein is required for poly(A)-binding protein-stimulated poly(A)-nuclease activity. *J. Biol. Chem.* **271,** 432–438
53. Martinez, J., Ren, Y. G., Thuresson, A. C., Hellman, U., Astrom, J., and Virtanen, A. (2000) A 54-kDa fragment of the poly(A)-specific ribonuclease is an oligomeric, processive, and cap-interacting poly(A)-specific 3′ exonuclease. *J. Biol. Chem.* **275,** 24222–24230
54. Zuo, Y., and Deutscher, M. P. (2002) Mechanism of action of RNase T. I. Identification of residues required for catalysis, substrate binding, and dimerization. *J. Biol. Chem.* **277,** 50155–50159
55. Uchida, N., Hoshino, S., and Katada, T. (2004) Identification of a human cytoplasmic poly(A) nuclease complex stimulated by poly(A)-binding protein. *J. Biol. Chem.* **279,** 1383–1391
56. Deutscher, M. P., Marlor, C. W., and Zaniewski, R. (1984) Ribonuclease T: new exoribonuclease possibly involved in end-turnover of tRNA. *Proc. Natl. Acad. Sci. U. S. A.* **81,** 4290–4293
57. Nguyen, L. H., Espert, L., Mechti, N., and Wilson, D. M., 3rd (2001) The human interferon- and estrogen-regulated ISG20/HEM45 gene product degrades single-stranded RNA and DNA in vitro. *Biochemistry* **40,** 7174–7179
58. Yanagida, M., Shimamoto, A., Nishikawa, K., Furuichi, Y., Isobe, T., and Takahashi, N. (2001) Isolation and proteomic characterization of the major proteins of the nucleolin-binding ribonucleoprotein complexes. *Proteomics* **1,** 1390–1404
59. Hayano, T., Yanagida, M., Yamauchi, Y., Shinkawa, T., Isobe, T., and Takahashi, N. (2003) Proteomic analysis of human Nop56p-associated pre-ribosomal ribonucleoprotein complexes. Possible link between Nop56p and the nucleolar protein treacle responsible for Treacher Collins syndrome. *J. Biol. Chem.* **278,** 34309–34319
60. Yanagida, M., Hayano, T., Yamauchi, Y., Shinkawa, T., Natsume, T., Isobe, T., and Takahashi, N. (2004) Human fibrillarin forms a sub-complex with splicing factor 2-associated p32, protein arginine methyltransferases, and tubulins α3 and β1 that is independent of its association with preribosomal ribonucleoprotein complexes. *J. Biol. Chem.* **279,** 1607–1614
61. Ginisty, H., Sicard, H., Roger, B., and Bouvet, P. (1999) Structure and functions of nucleolin. *J. Cell Sci.* **112,** 761–772
62. Hingorani, K., Szebeni, A., and Olson, M. O. (2000) Mapping the functional domains of nucleolar protein B23. *J. Biol. Chem.* **275,** 24451–24457
63. Henning, D., So, R. B., Jin, R., Lau, L. F., and Valdez, B. C. (2003) Silencing of RNA helicase II/Guα inhibits mammalian ribosomal RNA production. *J. Biol. Chem.* **278,** 52307–52314
64. Zhang, H., Wang, J. C., and Liu, L. F. (1988) Involvement of DNA topoisomerase I in transcription of human ribosomal RNA genes. *Proc. Natl. Acad. Sci. U. S. A.* **85,** 1060–1064
65. Horsey, E. W., Jakovljevic, J., Miles, T. D., Harnpicharnchai, P., and Woolford, J. L., Jr. (2004) Role of the yeast Rrp1 protein in the dynamics of pre-ribosome maturation. *RNA* **10,** 813–827
66. Ripmaster, T. L., Vaughn, G. P., and Woolford, J. L., Jr. (1992) A putative ATP-dependent RNA helicase involved in Saccharomyces cerevisiae ribosome assembly. *Proc. Natl. Acad. Sci. U. S. A.* **89,** 11131–11135
67. Dreyfuss, G., Kim, V. N., and Kataoka, N. (2002) Messenger-RNA-binding proteins and the messages they carry. *Nat. Rev. Mol. Cell Biol.* **3,** 195–205
68. Tacke, R., Tohyama, M., Ogawa, S., and Manley, J. L. (1998) Human Tra2 proteins are sequence-specific activators of pre-mRNA splicing. *Cell* **93,** 139–148
69. Raijmakers, R., Schilders, G., and Pruijn, G. J. (2004) The exosome, a molecular machine for controlled RNA degradation in both nucleus and

cytoplasm. *Eur. J. Cell Biol.* **83,** 175–183
70. Liu, Q., Greimann, J. C., and Lima, C. D. (2006) Reconstitution, activities, and structure of the eukaryotic RNA exosome. *Cell* **127,** 1223–1237
71. Dziembowski, A., Lorentzen, E., Conti, E., and Seraphin, B. (2007) A single subunit, Dis3, is essentially responsible for yeast exosome core activity. *Nat. Struct. Mol. Biol.* **14,** 15–22
72. Schilders, G., Raijmakers, R., Raats, J. M., and Pruijn, G. J. (2005) MPP6 is an exosome-associated RNA-binding protein involved in 5.8S rRNA maturation. *Nucleic Acids Res.* **33,** 6795–6804
73. Saveanu, C., Namane, A., Gleizes, P. E., Lebreton, A., Rousselle, J. C., Noaillac-Depeyre, J., Gas, N., Jacquier, A., and Fromont-Racine, M. (2003) Sequential protein association with nascent 60S ribosomal particles. *Mol. Cell. Biol.* **23,** 4449–4460
74. Sydorskyy, Y., Dilworth, D. J., Halloran, B., Yi, E. C., Makhnevych, T., Wozniak, R. W., and Aitchison, J. D. (2005) Nop53p is a novel nucleolar 60S ribosomal subunit biogenesis protein. *Biochem. J.* **388,** 819–826
75. de la Cruz, J., Kressler, D., Rojo, M., Tollervey, D., and Linder, P. (1998) Spb4p, an essential putative RNA helicase, is required for a late step in the assembly of 60S ribosomal subunits in Saccharomyces cerevisiae. *RNA* **4,** 1268–1281
76. Bezin, L. G. B., and Morales, A. C. (October 28, 2004) Method of calibration of reverse transcription using a synthetic messenger RNA (SmRNA) as an internal control. World Intellectual Property Organisation Patent WO/2004/092414